Proceedings of the XVth Symposium on Measuring Techniques in Transonic and Supersonic Flow in Cascades and Turbomachines at the Università degli Studi di Firenze, September 21st-22nd, 2000

Aerodynamic Influence Coefficients on an Oscillating Turbine Blade in Three-Dimensional High Speed Flow

Design of a New Annular Sector Cascade Test Rig at KTH

Vogt, D. M., Fransson, T. H.
The Royal Institute of Technology
Stockholm, Sweden
contact: damian@egi.kth.se
tel: +46-8-7907480

ABSTRACT

An experimental research project has been started at the Royal Institute of Technology to investigate aeroelastic phenomena in a generic turbine cascade. The expected results include time-dependent aerodynamic pressures and boundary layer characteristics of three-dimensional features on a vibrating turbine blade at realistic Mach and Reynolds numbers and reduced frequencies.
A new annular sector cascade test facility has been designed for the study with a non-rotating sector of typical low pressure turbine rotor blade profiles. The use of an annular rather than a linear shaped cascade leads to three-dimensional flow features as they are present in real turbines. One blade in the cascade can be made oscillating in a controlled 1st bending mode at different oscillation amplitudes and frequencies. A new type of mechanical oscillation mechanism has been designed with two co-rotating cylindrical cams as actuators. The mechanism covers continuously a wide range of oscillation amplitudes and frequencies.
This publication gives an overview over the planned experiments and describes the design of the test facility and the oscillation mechanism.

NOMENCLATURE

Symbols

c	blade chord
ecc	eccentricity
f	oscillation frequency
opd	operating distance
r	radius
v	flow velocity
z	axial coordinate
α	flow angle, sidewall angle
ϑ	circumferential angle
φ	oscillation angle

Subscripts

F	reference radius
ax	axial

INTRODUCTION

As the trend in modern turbomachinery design leads to increased flow temperatures and velocities at reduced weights of the structural components, aeroelastic phenomena become more and more important. In general, these phenomena can be divided by their nature into two groups; firstly self-excited vibrations also referred to as *flutter*, and secondly vibrations resulting from an external excitation referred to as *forced response*. Flutter occurs in a cascade at a certain flow velocity without any external excitation. The flutter frequency collides with the natural frequency of the mechanical cascade oscillation system.

The object of the present investigation is the coupling of the blades in a cascade during flutter by the fluid, referred to as aerodynamic coupling. Considering a fluttering cascade, the oscillation frequency and amplitude results from an energy exchange between the oscillating structure and the fluid. An oscillating blade acts thereby an influence on itself as well on its neighbors. A measure of the coupling of oscillating blades is given by aerodynamic influence coefficients representing a blade specific, phase related and non-dimensional blade surface pressure value. Aerodynamic influence coefficients can thus be employed to explain aerodynamic instabilities occurring in cascades.

The study aims towards obtaining experimentally determined aerodynamic influence coefficients in a cascade with one blade oscillating in an controlled 1st bending mode. Experimental investigations with oscillating blades have been carried through in both annular and linear cascades. Bölcs and Schläfli (1984), Bölcs, Fransson and Schäfli (1989) and Körbächer and Bölcs (1994) conducted experiments in a non-rotating annular turbine cascade. The advantage of this type of cascade is the inherent circumferential flow periodicity due to the absence of limiting sidewalls. A set of standard configurations acquired by Bölcs and Fransson (1986), Fransson and Verdon (1993) and Franson et al. (1998) in the named cascade are available for use in an experimental database. Poensgen and Gallus (1991) conducted experiments in an annular compressor cascade with one blade instrumented to measure the unsteady pressure. Buffum and Fleeter (1988) investigated aeroelastic phenomena in a linear cascade with all and with individual blades oscillating. Bell and He (1997) investigated the unsteady blade surface pressure on an oscillating blade in a linear cascade.

By using an annular sector cascade in the present study, realistic flow conditions shall be achieved, as three-dimensional flow features are present due to radial pressure gradients. The limitation of the circumferential extension of the cascade to a sector leads to a reduction of the needed mass flow, which allows the use of an already existing air supply system. However, circumferential flow periodicity is no longer inherently present and now has to be achieved by the shape of the flow duct. Low pressure turbine rotor blade profiles will be mounted in the cascade. Other than in a real engine where the inflow to the rotor is highly sheared over the span, the inlet flow angle will be constant due to the use of a sector shaped inlet duct.

The unsteady blade surface pressure will be measured on the oscillating as well as on one steady blade. Both the oscillating and the instrumented steady blade can be mounted at different positions in the cascade, which offers a large range of experimental flexibility.

PLANNED EXPERIMENTS

The foreseen experiments can be divided into steady and unsteady measurements. The steady measurements will be carried out to validate the flow conditions in the cascade to guarantee flow periodicity and to provide a comparative data set for CFD simulations. The unsteady measurements will provide the time-dependent blade surface pressure that finally will be combined to aerodynamic influence coefficients. Below, a list of the planned measurements is given:

- Global test rig performance including measurement of static and total pressure and temperature at different positions
- Steady wall pressure at hub and shroud up- and downstream (several axial positions)
- Steady wall pressure at shroud within the bladed section
- Steady multihole probe traverses up- and downstream
- Steady pressure distribution on the blade
- Unsteady wall pressure at hub and shroud up- and downstream (several axial positions)
- Unsteady wall pressure at shroud within the bladed section
- Unsteady pressure distribution on the oscillating and the steady blades
- Optical measurements within the blade passages for shock detection

DESCRIPTION OF THE TEST FACILITY

The test facility modifies an existing modular wind tunnel assembly that has been validated by Wiers (1999). Specific modules have been redesigned to fulfil the requirements for the present study such as providing the required inflow conditions, housing an oscillating blade and featuring the required experimental possibilities.

A continuously working screw compressor driven by a 1MW electrical motor supplies 4.75 kg/s air at 4bar and 120C. The compressed air can be cooled down to a minimum temperature of 30C. A set of valves up- and downstream of the test facility allows setting pressure level

and mass flow range, thus adjusting Mach and Reynolds number independently in a small range of approximately between Re_{cax} =3e5 and 5e5. Table 1 shows the set of nominal flow parameters used in the current study.

Parameter	Unit	Value
Inlet flow angle	°	26
Outlet flow angle	°	-61
Inlet Mach number	-	0.31
Outlet Mach number	-	0.82
Inlet total temperature	K	330
Inlet total pressure	Pa	1.6e5
Re_{cax}	-	3.7e5
Mass flow rate	kg/s	4.31

Table 1. Nominal flow parameters in the test cascade

Design of the Test Object

A new blade profile has been designed with characteristics of a typical highly loaded transonic low pressure turbine rotor blade. The design has been carried out matching the conditions in a real low pressure turbine stage of a jet engine and has then stepwise been transferred from real engine to test rig conditions. The steps included the application of constant boundary conditions, a non-rotating frame of reference and a geometrical scaling factor of 1.5. The nominal tip gap has been set to 1mm and can be varied within 0.5mm and 2mm.

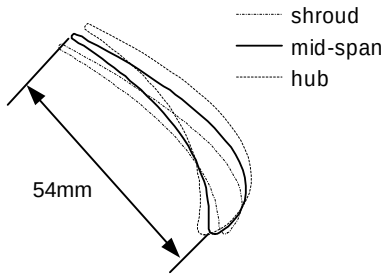

Figure 1. Scaled blade profile at hub, mid-span and shroud

The divergent hub shape that has been present in the original design has been replaced by a cylindrical shape to allow the blade oscillation. The new hub shape has been achieved by applying a cylindrical cut near the blade root of the original profile geometry. The resulting blade profile has an aspect ratio of 2.3 and an axial chord of 44mm. Figure 1 shows the final profile at hub, mid-span and shroud.

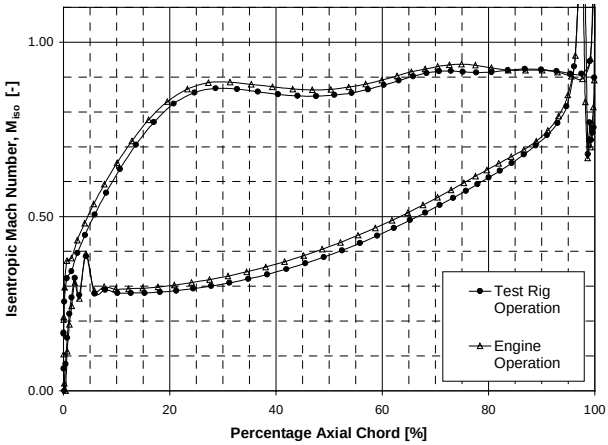

Figure 2. Isentropic profile Mach number distribution at mid-span; result from a 3D inviscid CFD analysis

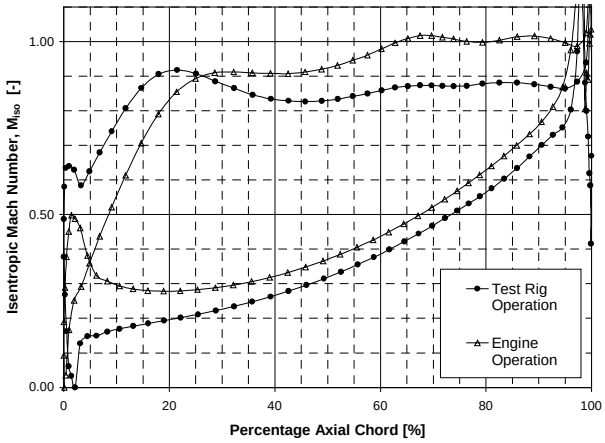

Figure 3. Isentropic profile Mach number distribution near shroud; result from a 3D inviscid CFD analysis

It has been seen from a CFD analysis that the major characteristics of the blade loading are preserved throughout the transformation from engine conditions to test rig operation, i.e. high loading over the entire span, transonic flow conditions and a slight deceleration on the suction side at 25% c_{ax}. It is assumed that the deceleration will lead to transition and thus to a well-defined transition point. Figure 2 and 3 show the loading at mid-span and near shroud respectively for the profile operated at real

engine and test rig conditions. Little difference can be seen in the loading at mid-span shown in Figure 2 for both operating conditions as the uniform inflow conditions in the test rig correspond to the conditions at mid-span in the engine. A large difference, however, can be seen at shroud as it is shown in Figure 3 that results from a different inflow angle at test rig operation than at engine operation.

Inlet Module

The fully assembled test facility is shown in Figure 6 denoting the different parts. The helicoidally shaped inlet part with annular sector cross section directs the flow towards the test section at the relative inflow angle of the investigated rotor blade. The inlet part is flanged to the contraction module in direction of the main cascade axis and deviates the flow from the axial to the inflow direction. The deviation is achieved by the bowed shape of the inlet part and is assisted by 4 vanes each of it made of a bowed plate.

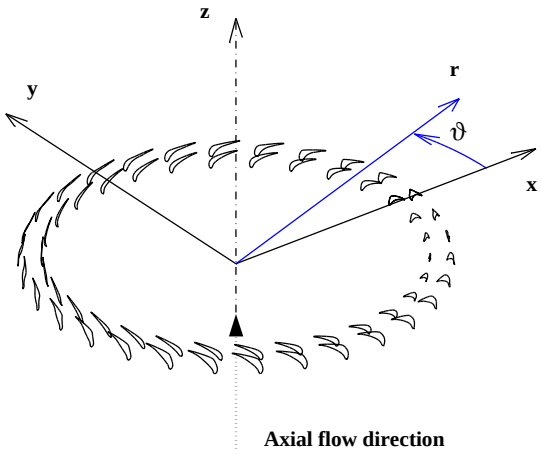

Figure 4. Coordinate convention

Two types of inlet modules have been developed during the redesign phase. One type conserves the cross-section as a true sector along the helicoidal length of the flow path and has both inlet and outlet flanges true sector shaped. This leads however to a spanwise distortion of the imposed inflow angle that amounts to –2.62° at hub and +2.5° at the shroud for an angle of 26° at the reference radius as it can be determined from Equation (1) following the coordinate conventions shown in Figure 4.

$$\alpha(r) = \arctan\left[\frac{r}{r_F}\tan(\alpha_F)\right] \quad \textbf{(1)}$$

To eliminate this distortion, another however more complicated inlet part has been designed with constant inclination of the sidewalls in the rϑ-z-plane over the span. The constant inclination of the sidewalls can be formulated to a condition that can be written as

$$\alpha(r) = \arctan\left[\frac{d\vartheta(r)}{dz}\right] \equiv const. \quad \textbf{(2)}$$

Other than the first type, this leads to a rhomboid sector shape of the inlet flange as it is showed in Figure 5, i.e. with no longer radial sidewalls as hub and shroud part are twisted relatively to each other. The difference of the two types of inlet modules lies in the manufacturing complexity that is considerably higher for the latter. However, this type has been chosen, as it intends to provide uniform and well-defined inflow conditions.

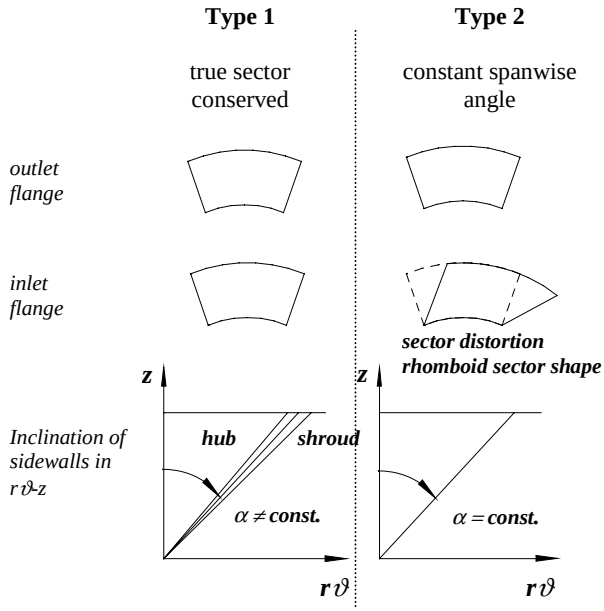

Figure 5. Inlet and outlet flange cross-sections for distortion affected and distortion free inlet modules

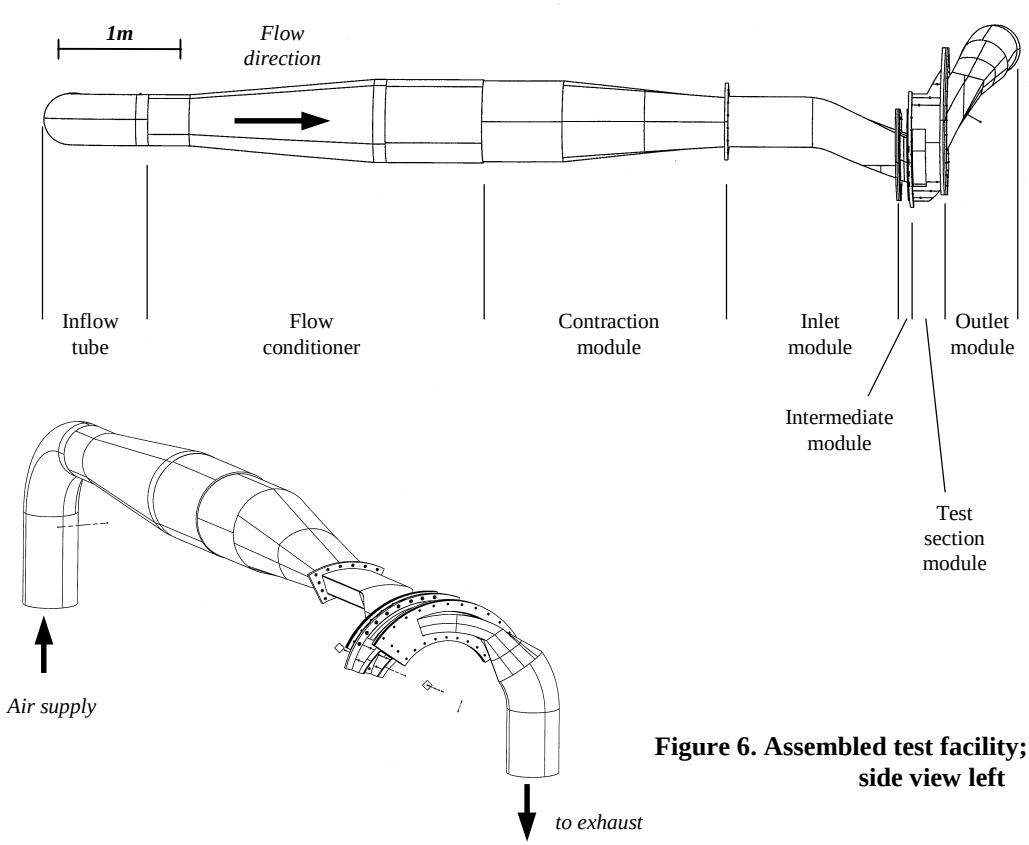

Figure 6. Assembled test facility; top view above, side view left

Intermediate Module

An intermediate module is flanged between the inlet and the test section module to provide the following possibilities each of it foreseen as a part of its own:

- Boundary layer cut-off upstream of the test section at hub and shroud
- Visualization of cascade inflow conditions
- Simulation of an upstream lying stator by introducing a pinwheel

Test Section Module

The test section module accommodates the blades and all installations for the planned flow measurements. The cascade extents over eight passages, housing in a first arrangement seven blades with one full passage on each side of the cascade as it is shown in Figure 7. A further arrangement would be with eight blades and a half passage on each side of the cascade.

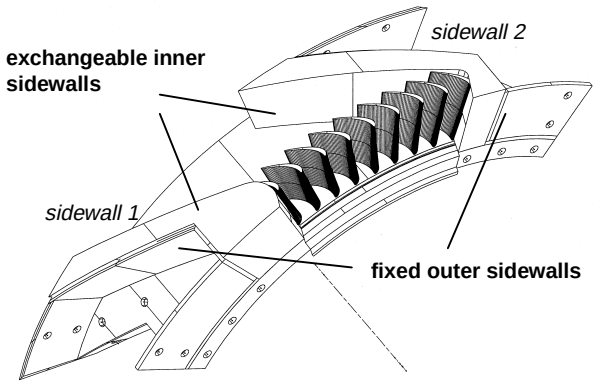

Figure 7. Test section of the annular sector cascade test facility, partially disassembled

The blades are mounted in a way that allows arbitrarily repositioning of each of the blades. The blades are mounted from the shroud through a slot in the shroud part that becomes accessible after having moved a slider that is integrated in the shroud part into its outermost position.
The blade oscillation is performed from below the hub and is not affecting the flow field in the cascade with intruding parts. The support of the oscillation mechanism is pivoted in the center of the cascade below the hub, which allows the oscillation mechanism to be moved to any blade position. Thanks to this arrangement, the influence coefficients can ideally be determined up to blade ±6 with 7 blades mounted in the cascade. Further restrictions of this range will in reality be dictated by the circumferential extension of steady periodic flow conditions as well as of the strength of unsteady pressure reflections from the sidewalls, which have to be determined experimentally at a later date.

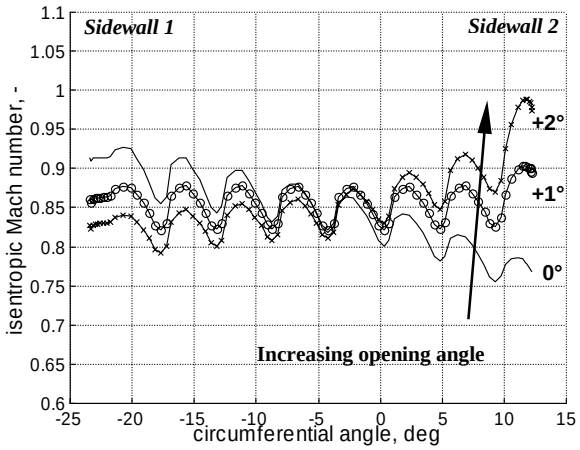

Figure 8. Influence of the inclination angle of sidewall 2 on the circumferential pressure distribution at 25% cax downstream of the cascade; results from a 3D Navier-Stokes CFD analysis on the redesigned test section

The sidewalls of the test section downstream of the cascade have been designed in a block-building manner incorporating that a pair of fixed outer sidewalls are assisted by a pair of exchangeable inner sidewalls as it is indicated in Figure 7. This gives the possibility to control the flow diffusion just downstream of the cascade by changing the geometrical configuration of the inner sidewalls. It is foreseen to have either sidewalls that are parallel in the rϑ-z-plane, diverging walls on either sides or a step diffuser by completely omitting the inner sidewalls. A flexible sidewall has been conceptualized that shall cover continuously a certain range of tangential inclination angles while withstanding a tangential force. This type of wall has however not yet reached prototyping stage and practical performance has thus not yet been tested.
A pair of slot-treated inner sidewalls will be used in case of shock reflection should appear downstream of the cascade during blade oscillation.

It has been seen from an ongoing full-scale 3D CFD analysis on the test section and the adjacent parts that the inclinations in the rϑ-z-plane of the sidewalls downstream play a crucial role in controlling the circumferential flow periodicity within the cascade. By opening either wall, a controlled diffusion can locally be initiated leading to a suction effect downstream of the cascade and a redistribution of the static pressure field. The potential of controlling the periodicity by means of the described arrangement can be seen in Figure 8, showing the influence of the inclination angle of sidewall 2 on the circumferential isentropic Mach number distribution downstream. Whereas the velocity level decreases in the circumferential direction from sidewall 1 to sidewall 2 in case of 0° opening angle, the velocity distribution becomes equalized by increasing the opening angle of sidewall 2 to +1°. Further opening leads to higher velocity near sidewall 2 and thus to an unbalanced flow field downstream of the cascade. The presented results predict that the flow will be very sensitive to the sidewall configuration downstream of the cascade as small changes in the wall inclination seem to have a large impact on the circumferential flow periodicity.

Outlet Module

The outlet module is made of a helicoidally shaped diffuser with an annular sector cross section followed by a bowed settling chamber of circular cross section. Similar to the downstream part of the test section, the diffuser is built up of a pair of fixed outer walls and a pair of exchangeable inner sidewalls to control flow diffusion.

Instrumentation

The wall pressure within the cascade at hub and shroud is measured by means of pressure taps that are integrated in traversable sliders. Each slider is made of a segment of a profiled ring and is carried in the hub and shroud plate

respectively by rails as it is shown in Figure 9. The sliders have an actuation range of half the opening angle of the cascade in the circumferential direction thus allowing a complete traverse of the wall pressure at one axial position with just two pressure taps. By measuring with several pressure taps per axial position simultaneously, the data acquisition process can be speeded up considerably.
Depending on the nature of the measurement, there will be sliders equipped with either static pressure taps or fast response pressure transducers. The sliders in the hub part can be exchanged arbitrarily, which reduces the amount of instrumentation needed. All sliders are sealed by means of Teflon tubes in the axial gap as it is shown in Figure 9 to eliminate leakage flows. A probe supporting unit with one degree of freedom can be connected to the slider in the shroud wall at different axial positions for probe traverses in radial and circumferential direction. The slider thus eliminates the sealing problem that otherwise would be present due to having an open slot in the shroud.

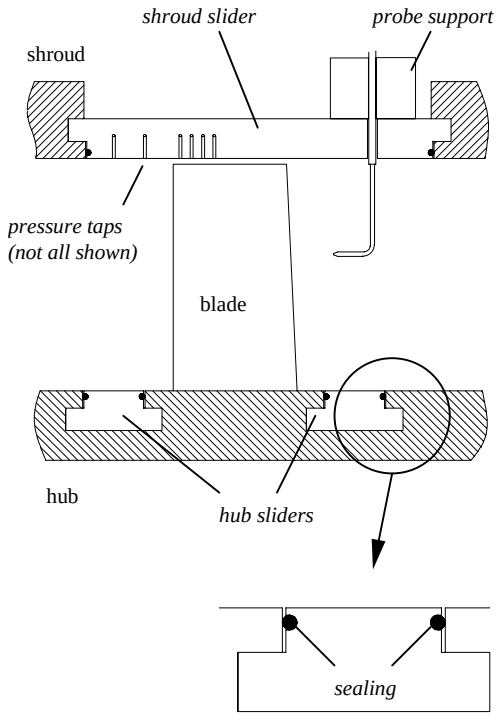

Figure 9. Schematic view of the test section showing the position and the geometry of the measurement sliders

The material of the sliders is Teflon, which leads to a minimized friction under absence of lubrication in combination with the hub and shroud plates made of steel. The actuation of the sliders in the circumferential direction is performed individually for each of the three sliders by means of stepping motors and a closed loop notch belt allowing operation in either direction. Figure 10 shows the principle of the slider actuation. The position of each slider is controlled by the pulse signal of the stepping motor assisted by an arrangement of electrical contacts. The latter consists of a number of needle contacts embedded into the respective slider rail and arranged in 3 different lanes providing a non-ambiguous and direction dependend position signal. The signal serves as a feedback signal into the position control loop and as reference points during calibration.

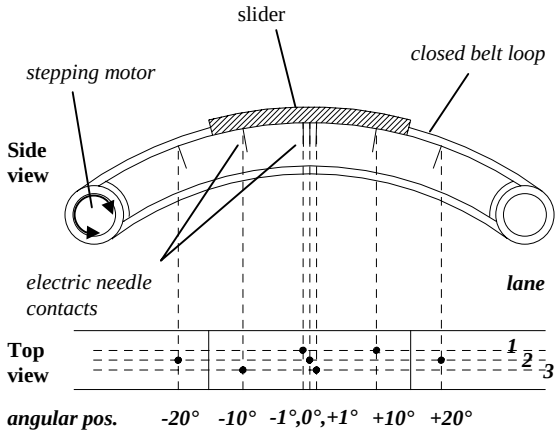

Figure 10. Sketch of the measurement slider actuation and the feedback contact positioning

A number of blades will be instrumented for either steady or unsteady pressure measurements. Measurements of the chordwise static pressure have been foreseen at three different spanwise positions with a resolution per spanwise location of 20 points (SS and PS) for the steady and 10 points for the unsteady measurements. For the unsteday measurements, fast response pressure transducers (KULITE, LQ series, natural frequency > 300kHz) are foreseen being mounted from the back into a milled cavity with a tap extending to the measurement position. The size of the cavity will be determined such that the resonance frequency of the assembly is much higher than the maximum frequency of the expected aerodynamic phenomena. The feeding wires of the sensors will be

directed to the blade root within radially directed milled slots and covered by an Epoxy resin.
Thanks to the interchangeable way of mounting the blades, the planned results can be acquired with each a blade instrumented for steady and unsteady measurements.

Data Acquisition

For the steady measurements a multichannel pressure measurement system with 208 channels (PSI 8400) will be used. The unsteady data will be acquired with a high-speed digital recording system (Kayser Threde K8000). The system features 32 channels each being equipped with a DC Bridge amplifier and has a bandwidth of 100kHz. In addition to the unsteady pressure data, a TTL signal from the oscillation actuator as well as the signal from a accelerometer embedded into the oscillating blade will be recorded for triggering and control reason.

DESIGN OF THE OSCILLATION MECHANISM

Requirements

Typical reduced frequencies of transonic bending flutter are in the range of 0.25 to 0.5 based on the half chord. The aim has therefore been set up for the present study to oscillate the blade at reduced frequencies from 0.1 to 0.5. From the expression for the reduced frequency based on half chord, given in Equation (3), a maximum oscillation frequency of 500Hz has been determined.

$$k = \frac{2\pi f}{v_{ax}} \cdot \frac{c_{ax}}{2} \qquad \textbf{(3)}$$

A listing of the oscillation conditions that shall be achieved with the oscillation mechanism is given below:

- Mode : 1st bending
- Amplitude : variable 0º…10º
- Frequency : variable 0…500Hz
- Shape : sinusoidal
- Direction : natural ±5º

The above listed upper limits of the planned amplitude and frequency range will not be achieved simultaneously as material stresses increase considerably in the oscillating parts with both oscillation amplitude and frequency. Possible oscillation operating points will be between low frequency/high amplitude and high frequency/low amplitude parameter couples.
The bending axis will be located at a small distance of about 8mm below the blade hub. It is foreseen to allow different bending axis directions in a range of ±5º from the natural bending axis direction of the blade.

Oscillation Principle

The oscillating blade is pivoted below its root with a globe bearing and is provided with a lever emerging below the hub towards the center of the machine. The controlled 1st bending oscillation is generated by a mechanism acting with an alternating force on the lower end of the lever.
A sketch of the blade oscillation principle is shown in Figure 11.

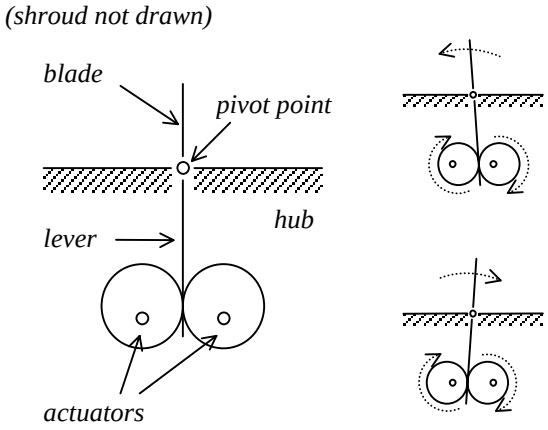

Figure 11. Principle of the controlled blade oscillation and the oscillation actuators; two extreme positions shown on the right hand side

Description of the Mechanism

This mechanism consists of two circular cams that are placed on each side of the lever and are co-rotating around an eccentric pivot at the same rotational speed.

The actuator cams are ideally non-circular, but slightly egg-shaped, which results from the requirement of achieving a sinusoidal oscillation shape and the cinematic of the presented mechanism with a lever moving as a pendulum. However, the cams have been chosen circular which allows the use of roller bearings to reduce friction between the actuator and the lever. The fact of non-

circularity has been taken into consideration by placing a layer of elastic compensation material around the actuators.

To avoid flow deterioration around the oscillating blade, the blade root is equipped with an elastic sealing allowing oscillations at the planned parameters. The use of a globe bearing rather than a roller bearing gives the possibility of oscillating the blade around different bending axis directions by turning the oscillation mechanism around the lever axis.

Whereas the oscillation frequency is direct proportional to the rotational speed of the actuator cams, the oscillation amplitude depends on the following geometrical parameters, which are shown in Figure 12:

- The eccentricity of the cams
- The operating distance, i.e. the normal distance from the blade pivot point to the axis of rotation of the cams

A first version of the mechanism of the above presented type will cover continuously a range in amplitude of between 0deg and 11deg. The maximum oscillation frequency, however, is limited to 250Hz due to the upper speed limit of the roller bearings used to minimize friction between the actuators and the actuation lever. An increase of the maximum oscillation frequency will be taken into consideration after this actuation concept has shown reliable performance in practice. Possible ways of increasing the upper frequency limit could be the use of different roller bearings (low potential expected), the use of a different type of bearing such as oil film or air film bearings (high potential expected).

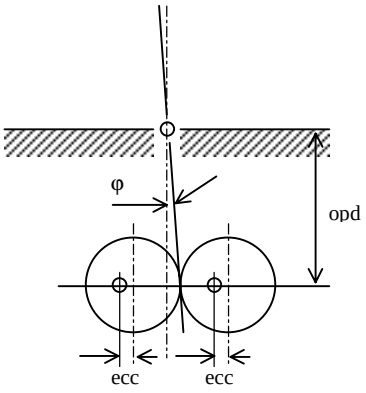

Figure 12. Parameters of the oscillation mechanism determining the oscillation amplitude

The continuity in oscillation amplitude is achieved by keeping both the eccentricity of the cams as well as the operating distance variable. The eccentricity of the cam is varied by means of a double eccentric support as it is shown in Figure 13. It is crucial for the proper operation of the oscillation mechanism to always have the identical eccentricity for both actuators. This lead to a design that restricts changing the eccentricity within discrete predefined steps by means of an indexing mechanism as it is shown in Figure 13.

The described variation of the eccentricity leads to a discrete change in oscillation amplitude. By continuously varying the operating distance of the actuator, a fine adjustment of the resulting amplitude can be performed at each chosen eccentricity. The support of the oscillation actuators has therefore been designed in a way that allows shifting the actuators radially in- and outwards. Furthermore the actuation mechanism can be rotated around its own axis, which gives the possibility of changing the direction of the bending axis.

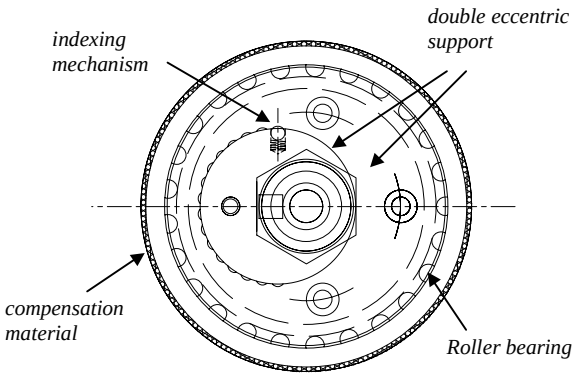

Figure 13. Oscillation actuator allowing a stepwise variation of the eccentricity

The actuation mechanism has been designed in a way that provides balancing for all rotating parts regardless of the eccentricity chosen. The balancing is achieved independently for each actuator by two counterweights placed on the same axis on either side and pivoted at the same arbitrarily directed eccentricity. By changing the eccentricity of the actuator, the counterweights are automatically repositioned by means of an integrated gear drive.

Both actuators are driven by a common belt drive and one frequency controlled asynchronous electrical motor as it is shown in Figure 14. The drive axis of the motor is aligned with the machine axis of the cascade. This allows repositioning the oscillation mechanism to any of the blade positions by just removing the upper fixation at the hub and rotating the mechanism to its new position.

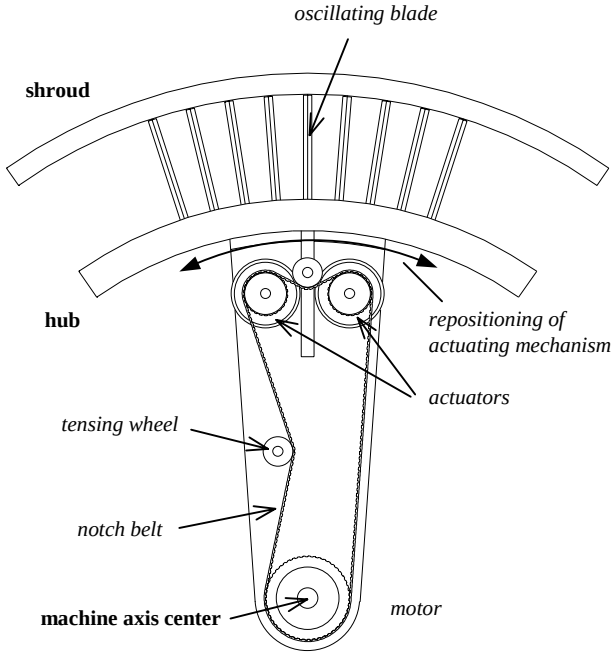

Figure 14. Sketch of the oscillation drive mechanism

Oscillation Control Unit

The blade oscillation is foreseen being controlled by the following two input signals:

- A TTL-signal from the actuator drive loop
- An acceleration sensor placed in the oscillating blade

The TTL-signal from the oscillation actuator drive loop will be generated optoelectronically with a specially shaped disk rotating inbetween a light source – light detector assembly. The rotating disk will be shaped to generate one pulse per rotation. An acceleration sensor embedded into the blade will be used to determine the oscillation shape.

CONCLUSIONS

The design of a new annular sector cascade test facility for the investigation of aeroelastic phenomena has been presented. A typical low pressure rotor blade profile will be used as such profiles are naturally susceptible to blade flutter. The investigated blade profiles will be mounted in a non-rotating annular sector cascade whereas one blade can be made oscillating in a controlled 1st bending mode. The test section will be built in a modular way, which shall allow a direct control of the flow periodicity in the cascade. Results from a full scale 3D CFD analysis on the test section predict that flow periodicity is heavily influenced by the configuration of the sidewalls downstream of the cascade.
The oscillating blade will be pivoted at its root and oscillated as a rigid body. A new type of mechanical oscillation mechanism has been designed for the study. The mechanism operates with two co-rotating eccentric cams and covers continuously a large range of bending amplitude.

A major limitation with the presented setup has been identified on the aerodynamic side. The absence of a centrifugal force field and the constant inflow direction to the cascade lead to a changed spanwise blade loading compared to operation at real engine conditions. Results of a CFD analysis on the cascade allowed a quantification of the named difference in the blade loading distribution and showed that the characteristic of the loading as it is present at engine conditions is preserved in the experiment. The difference is justified by the fundamental nature of the study that aims to provide information for the further understanding of a phenomenon rather than the determination of a real aeroelastic behaviour.

First tests with the presented test facility are foreseen in the first half of year 2001.

ACKNOWLEDGEMENTS

The authors would like to thank the Swedish Gas Turbine Center (GTC) for the promotion of the present study.

REFERENCES

Bell, D. L., He, L., 1997, "Three Dimensional Unsteady Pressure Measurements for an Oscillating Turbine Blade", ASME Paper 97-GT-105

Bölcs, A., Schläfli, D., 1984, "Flutter Phenomena in a Transonic Turbine Cascade", Proceedings of the Unsteady Aerodynamics of Turbomachines and Propellers Symposium, Cambridge, England, September, pp. 411-425

Bölcs, A., Fransson, T. H., Schläfli, D., 1989, "Aerodynamic Superposition Principle in Vibrating Turbine Cascades", AGARD, 74th Specialists' Meeting of the Propulsion and Energetics Panel on Unsteady Aerodynamic Phenomena in Turbomachines, Luxembourg, August 28 – September 1

Bölcs, A., Fransson, T. H., 1986, "Aeroelasticity in Turbomachinery: Comparison of Theoretical and Experimental Cascade Results", Air Force Office of Scientific Research, AFOSR-TR-87-0605

Buffum, D. H., Fleeter, S., 1988, "Investigation of Oscillating Cascade Aerodynamics by an Experimental Influence Coefficient Technique", AIAA Paper 88-2815

Fransson, T. H., Verdon, J. M., 1993, "Panel Discussion on Standard Configurations for Unsteady Flow Through Vibrating Axial-Flow Turbomachine Cascades", Unsteady Aerodynamics, Aeroacoustics and Aeroelasticity of Turbomachines and Propellers, H. M. Atassi, ed., Springer Verlag, New York, pp. 859-889

Fransson, T. H., Jöcker, M., Bölcs, A., Ott, P., 1998, "Viscous and Inviscid Linear/Nonlinear Calculations Versus Quasi 3D Experimental Cascade Data for a New Aeroelastic Turbine Standard Configuration", ASME Paper 98-GT-490

Körbächer, H., Bölcs, A., 1994, "Experimental Investigation of Unsteady Behavior of a Compressor Cascade in an Annular Ring Channel", Paper presented at the 7th ISUAAT Conference in Fukuoka, Japan, September

Poensgen, C. A., Gallus, H. E., 1991, "Experimental Investigation on the Unsteady Pressure Field on a Vibrating Cascade in Unsteady Flow", presented at Unsteady Aerodynamics of Turbomachines and Propellers, University of Notre Dame, Indiana, September 15-19, pp. 583-601

Wiers, S.-H., 1999, "Design and Validation of an Annular Sector Cascade Facility", Licentiate Thesis KTH Stockholm, ISBN 91-7170-498-1